Computational Studies of the Thermochemistry for Conversion of Glucose to Levulinic Acid

Rajeev S. Assary,[†,⊥] Paul C. Redfern,[‡] Jeff R. Hammond,[∥] Jeffrey Greeley,[§] and Larry A. Curtiss*[,†,§]

Materials Science Division, Argonne National Laboratory, Argonne, Illinois 60439, Chemical Sciences and Engineering Division, Argonne National Laboratory, Argonne, Illinois 60439, Center for Nanoscale Materials, Argonne National Laboratory, Argonne, Illinois 60439, Argonne Leadership Computing Facility, Argonne National Laboratory, Argonne, Illinois 60439, and Chemical & Biological Engineering, Northwestern University, Evanston, Illinois 60208

Received: February 15, 2010; Revised Manuscript Received: May 18, 2010

The thermochemistry of the conversion of glucose to levulinic acid through fructofuranosyl intermediates is investigated using the high-level ab initio methods G4 and G4MP2. The calculated gas phase reaction enthalpies indicate that the first two steps involving water molecule elimination are highly endothermic, while the other steps, including additional water elimination and rehydration to form levulinic acid, are exothermic. The calculated gas phase free energies indicate that inclusion of entropic effects makes the dehydration steps more favorable, although the elimination of the first water is still endothermic. Elevated temperatures and aqueous reaction environments are also predicted to make the dehydration reaction steps thermodynamically more favorable. On the basis of these enthalpy and free energy calculations, the first dehydration step in conversion of glucose to levulinic acid is likely a key step in controlling the overall progress of the reaction. An assessment of density functional theories and other theoretical methods for the calculation of the dehydration and hydration reactions in the decomposition of glucose is also presented.

1. Introduction

Catalytic or thermal conversion of biomass to fuels and useful chemicals is vital to current and future energy needs and industrial development. Basic chemical transformations that enable this conversion are hydrolysis of cellulose to carbohydrates and subsequent selective dehydration, rehydration, hydrogenation, condensation, and oxidation to lead to various hydrocarbons. Recent research[1−6] on the catalytic conversion of carbohydrates to liquid alkanes (C_3-C_7) and useful industrial chemicals such as 5-hydroxy methyl furfural, levulinic acid, and furfural highlight developments in this area. Design of more efficient catalysts and new insights into the kinetics and thermodynamics of these basic chemical transformations still remain a challenge. Accurate information on the energetics for these processes is an important aspect of addressing these challenges. Advanced quantum chemical methods and faster computers are enabling the prediction of accurate energetics of chemical transformations of the larger molecules involved in the processes.

Most of the previous theoretical studies have been aimed at determining the structures of carbohydrates, their conformational analysis, and calculation of their interaction energies with other hydrocarbons.[7−15] Also, kinetic modeling of glucose decomposition at different acid conditions and formations of levulinic acid from glucose[16,17] has been reported. However, accurate energetics for selective dehydration or rehydration of carbohydrates required to design appropriate catalysts have not yet, as far as we are aware, been reported.

In this work, we report on a quantum chemical evaluation of the energies for dehydration of glucose through fructofuranosyl intermediates to produce 5-hydroxy-methyl furfural (HMF), followed by rehydration of HMF to levulinic acid and formic acid; this is considered to be a key pathway for biomass coversion.[1,2] The steps involved in this glucose decomposition mechanism are shown in the reaction scheme in Figure 1. We have employed the Gaussian-*n* series of theory[18−23] including G3MP2//B3, G4MP2, and G4, to calculate the reactions energies for this pathway. We also assess the performance of several popular density functional theoretical (DFT) methods, including B3LYP, B3PW91, PW91, PBE, with Gaussian basis sets, and the PW91 and RPBE functionals with plane wave basis sets against the performance of the G4 theory. Additionally, the effects of various conformations of glucose, the effect of the reaction environment and temperature are included. Finally, calculated enthalpies of formation for the products, reactants, and intermediates are reported.

2. Computational Methods

The Gaussian-4 (G4) theory[22] was developed with the goal of calculating molecular energies within chemical accuracy. G4 theory has an average absolute deviation from experiment of 0.83 kcal/mol from an assessment on the 454 energies in the G3/05 test set composed of enthalpies of formation, ionization energies, electron affinities, proton affinities, and hydrogen bond energies.[21] We have employed the G4 level of theory to understand the enthalpy and free energy of the glucose decomposition reaction scheme investigated in this paper. We have also used two other Gn methods, based on reduced-order perturbation theory, in calculations on the glucose decomposition reaction. The first is G4MP2,[18] which is an alternative to the

* To whom correspondence should be addressed. E-mail: curtiss@anl.gov.
† Materials Science Division, Argonne National Laboratory.
⊥ Chemical & Biological Engineering, Northwestern University.
‡ Chemical Sciences and Engineering Division, Argonne National Laboratory.
∥ Argonne Leadership Computing Facility, Argonne National Laboratory.
§ Center for Nanoscale Materials, Argonne National Laboratory.

10.1021/jp101418f
Published on Web 06/24/2010

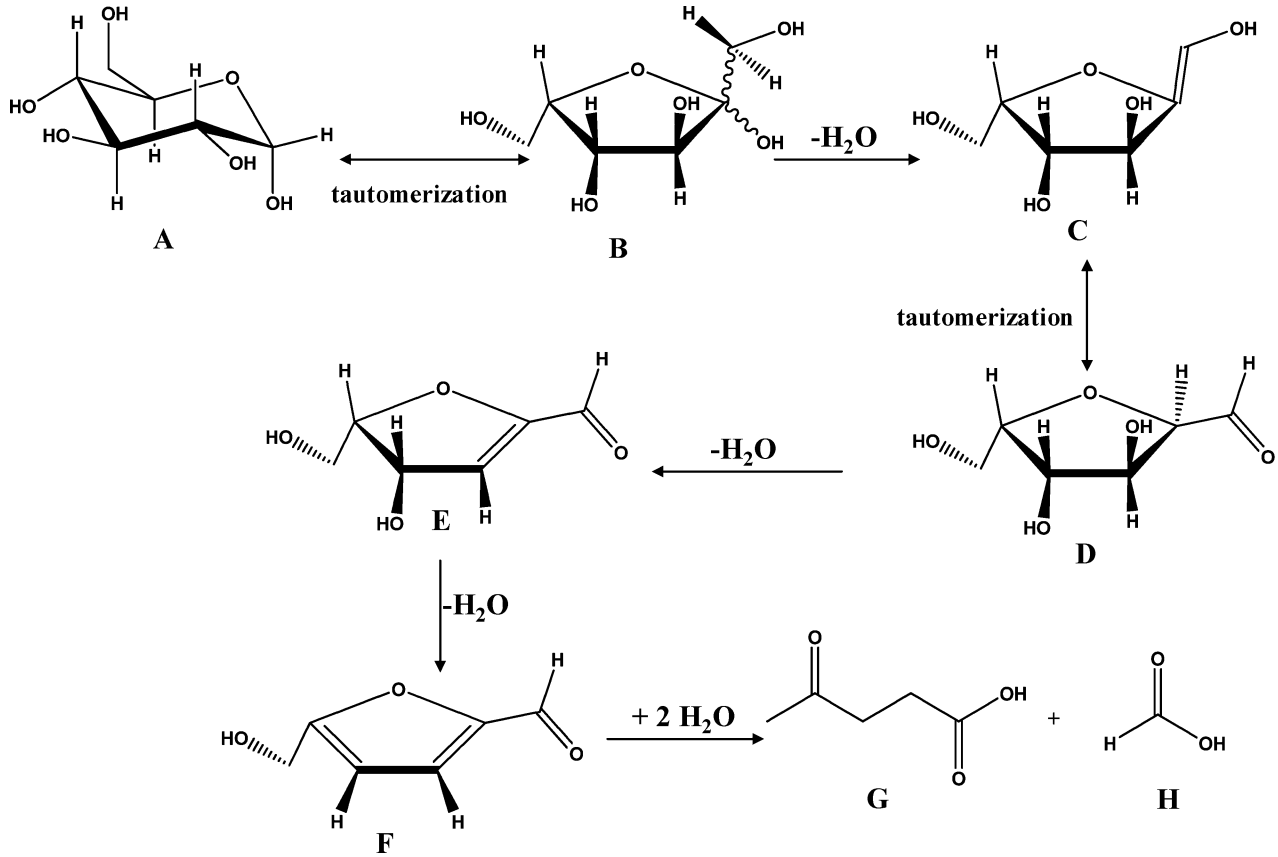

Figure 1. Schematic diagram of reactions investigated in this work. The labels A−H are as follows: A: α-D-glucose; B: β-D-fructose; C: enol intermediate produced by the initial dehydration; D: keto-intermediate produced after the tautomerization of species C; E: intermediate species formed after the removal of one water molecule from species D; F: hydroxy-methyl-furfural; G: levulinic acid; and H: formic acid.

computationally demanding G4 method, and second is G3MP2//B3,[19] which is an alternative to G3//B3 theory. The geometries and zero-point energies (scaled by 0.9854) for the G4 method were calculated at the B3LYP/6-31G (2df,p) level of theory. Thermal corrections were assessed at 298 and 448.15 K to investigate temperature affects on the free energies and enthalpies of reaction. The single point MP4/6-31G(2df,p) energies were calculated using 10f functions instead of 7f as in the published G4 methodology[22] due to the use of the NWCHEM code for these calculations.[24] The higher level correction parameters were rederived for this change and are available in the Supporting Information (Table S4). In order to account for the effects of the aqueous environment, calculations were also performed using a polarizable continuum model[25−27] (C-PCM) with the dielectric constant equal to water and UAKS atomic radii at the B3LYP/6-31G(2df,p) level of theory.

We have not carried out an accurate conformational analysis of the molecular species involved in the reaction mechanisms. This would require a detailed study due to the large number of conformations possible for species such as glucose and fructose. Instead, we have selected conformers based on the investigations of Momany et al.[12,28] who have computed the geometries and energetics of the low lying conformations of glucose. We have used their lowest energy conformer for glucose in our calculations on glucose and for the subsequent structures resulting from the dehydration steps and tautomerization steps. The conformers from Momany et al. were also used in calculations of the enthalpies of formation in Section 3.4.

In the assessments on density functional theory we calculated the reaction energies using the B3LYP functional with four basis sets 6-31G*, 6-31+G*, 6-311++G**, and/6-31G(2df,p) and optimized the geometry with each basis set. The B3LYP/6-31+G* geometries were used in single point energy calculations with a larger basis set, B3LYP/6-311+G(3df,2p)//B3LYP/6-31+G* and second-order perturbation theory, MP2/6-311+G(3df,2p)// B3LYP/6-31+G*. The latter method was also used on the B3LYP/6-31G(2df,p) optimized geometries, MP2/6-311+G(3df,2p)//B3LYP/6-31G(2df,p). In addition, calculations have also been performed using the PW91,[29] RPBE,[30] PBE,[31] and B3PW91[32,33] functionals. The first two functionals, PW91 and RPBE, were done periodically using the Dacapo code with full geometric optimization in both cases.[30] Ionic cores are described by ultrasoft pseudopotentials,[34] and the Kohn−Sham one-electron valence states are expanded in a basis of plane waves with kinetic energy below 340 eV; a density cutoff of 500 eV is used. To minimize interactions between mirror periodic images, an $18 \times 22.5 \times 15$ Å^3 unit cell, sampled only at the Γ point, was used. In all cases, convergence of the total energy with respect to the cutoff energies and the k point set is confirmed. The self-consistent RPBE and PW91 densities are determined by iterative diagonalization of the Kohn−Sham Hamiltonian, Fermi population of the Kohn−Sham states (kBT = 0.01 eV), and Pulay mixing of the resulting electronic density.[35] All total energies have been extrapolated to kBT = 0 eV. We note that the plane wave methods are popular for studies of catalytic surface calculations and this study provides an assessment of their use in future investigations.

The calculations for this investigation were done using the using Gaussian 03,[36] NWCHEM,[24] and DACAPO[30] (see above) software.

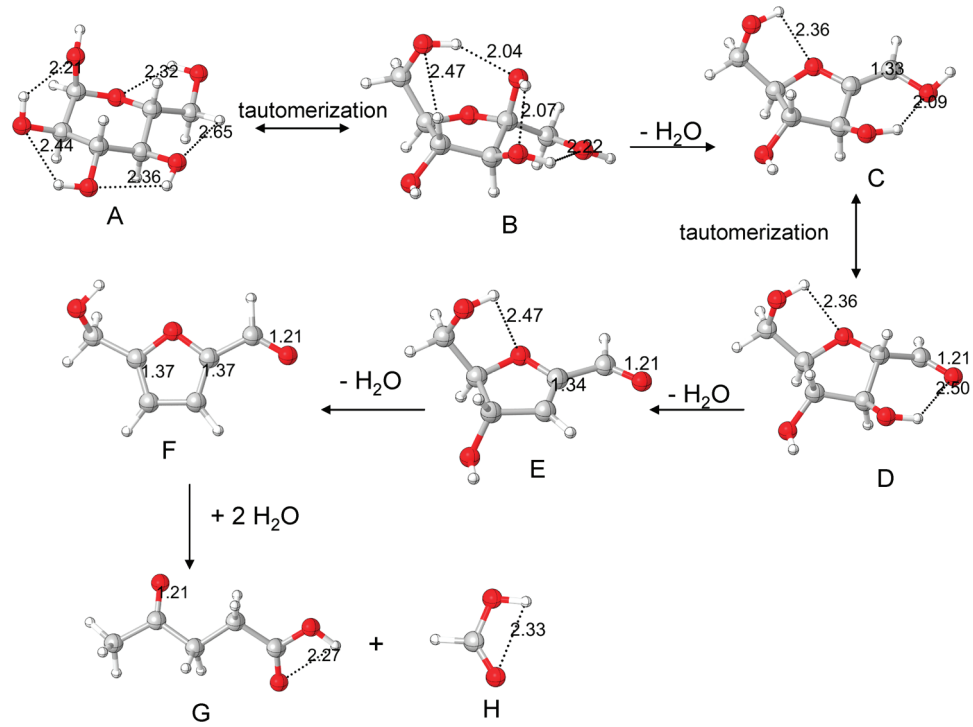

Figure 2. Optimized geometries at B3LYP/6-31G(2df,p) level of theory. Labels explained in Figure 1.

3. Results and Discussion

Calculations were carried out on the reaction scheme shown in Figure 1. In the first step, α-D-glucose (**A**) undergoes tautomerization to β-D-fructose (**B**) followed by removal of three water molecules to form HMF (**F**). Removal of the first water molecule from β-D-fructose leads to the enol-intermediate (**C**), which undergoes tautomerization to the aldo form (D). This is followed by removal of a second water molecule to form species **E**. Elimination of the third water molecule leads to HMF. Rehydration of HMF by two water molecules leads to levulinic acid (**G**) and formic acid (**H**). B3LYP/6-31G (2df,p) optimized molecular geometries of the species in this reaction scheme are presented in Figure 2. Predicted thermochemical data, including reaction energies (with and without zero-point energy corrections), enthalpies, and free energies at various levels of theory for the six reaction steps in this pathway are given in Table 1. In the following sections, we first discuss these results in more detail, following which we analyze solvation effects on the energetics, perform an assessment of other theoretical methods, and finally predict enthalpies of formation for the species in the reaction scheme.

3.1. Gas Phase Reaction Enthalpies and Free Energies. The G4 gas phase reaction enthalpy changes at 298 K from Table 1 for the glucose decomposition scheme (Figure 1) are shown in a schematic representation in Figure 3. The results indicate that the calculated enthalpy change associated with the conversion of α-D-glucose to β-D-fructose is 2.1 kcal/mol. Removal of the first water molecule from **B** to form **C** is calculated to be a highly endothermic process (+21.5 kcal/mol). This high endothermicity can be rationalized by simple bond breaking and making arguments. In fructose, two single bonds (C−O and C−H) are broken; in the dehydration products a single bond (C−C) becomes a double bond (C═C) in structure C and an O−H bond (H_2O) is formed. The single to double bond change costs energy, contributing to the high endothermicity. In addition, loss of intramolecular hydrogen bonding in going to structure C will cost some energy. The tautomerization from the enol (**C**) to aldo form (**D**) is an exothermic process; the calculated enthalpy change is −8.1 kcal/mol. Similar to the first dehydration step, the removal of a second water molecule from **D** to form **E** is also endothermic, by +7.6 kcal/mol. The lowering of the endothermicity in the second dehydration step is due to a conjugation between the ring C═C bond with the aldehyde C═O bond, which is not present in the first dehydration step. The enthalpy change upon the elimination of a third water molecule to form HMF (**F**) from **E** is −8.6 kcal/mol, where the exothermicity is predominantly due to the formation of the stable aromatic furan ring in HMF. The enthalpy of the rehydration reaction resulting in formation of levulinic acid and formic acid is highly exothermic (−38.6 kcal/mol).

Calculations at a higher reaction temperature (448 K) have little effect on the enthalpy change for conversion of glucose to fructose or for the keto−enol tautomerization process compared to the 298 K results as shown in Figure 3. However, there is a small change in the reaction enthalpy for the dehydration steps: the endothermicity is reduced by 1.7 and 1.5 kcal/mol, respectively, for the first two dehydration processes and the exothermicity is increased by 1.3 kcal/mol for the third dehydration. In addition, the exothermicity is reduced by 1.2 kcal/mol upon increase in temperature for the rehydration process.

The G4 gas phase free energy changes at 298 K from Table 1 for the glucose decomposition scheme (Figure 1) are shown in a schematic representation in Figure 4. The free energy change during the tautomerization steps is similar to the enthalpic change; however, the thermodynamic feasibility of the dehydration steps is quantitatively different from that of the enthalpy changes due to the entropic effects. The changes in the free energies for the dehydration processes are +9.2, −3.9, and −19.6 kcal/mol respectively for the first, second and third dehydration processes. The calculated free energy change of the rehydration process is −31.5 kcal/mol. Thus, from the free energy perspective, apart from the glucose−fructose tautomer-

TABLE 1: Thermochemistry (in kcal/mol) of Various Reactions Investigated Using Different Levels of Theory[a,b]

	reaction 1				reaction 2				reaction 3			
method	ΔE_e	ΔE_0	ΔH_{298K}	ΔG_{298K}	ΔE_e	ΔE_0	ΔH_{298K}	ΔG_{298K}	ΔE_e	ΔE_0	ΔH_{298K}	ΔG_{298K}
B3LYP/6-31G*	1.4	0.8	0.9	0.7	29.3	24.4	26.2	13.8	−11.1	−11.3	−10.7	−19.4
B3LYP/6-31+G*	2.3	1.7	1.8	1.5	23.4	18.7	20.4	8.0	−10.2	−10.4	−10.4	−10.9
B3LYP/6-311++G**	2.5	1.7	1.9	1.5	17.8	13.3	15.0	2.8	−6.9	−7.3	−7.3	−7.8
B3LYP/6-31G(2df,p)	0.7	0.2	0.2	0.0	24.7	20.1	21.8	9.6	−7.2	−7.6	−7.6	−8.1
B3LYP/6-311+G(3df,2p)// B3LYP/6-31+G*	2.5	1.9	2.0	1.7	16.7	12.0	13.7	1.3	−6.5	−6.7	−7.20	−10.4
MP2/6-311+G(3df,2p)// B3LYP/6-31+G*	2.3	1.7	1.8	1.5	26.1	21.3	23.0	10.7	−8.6	−8.8	−8.7	−9.2
MP2/6-311+G(3df,2p)// B3LYP/6-31G(2df,p)	2.5	1.9	2.0	1.7	26.0	21.4	23.1	10.9	−8.6	−9.0	−8.9	−9.4
G3MP2B3	6.1	5.3	5.6	4.5	20.6	16.3	17.7	6.4	−7.6	−7.8	−7.8	−8.2
G4MP2	2.8	2.2	2.3	2.05	23.4	18.9	20.5	8.3	−7.5	−8.0	−7.9	−8.4
G4	2.6	2.0	2.1	1.9	24.3	19.8	21.5	9.2	−7.8	−8.2	−8.1	−8.6
	reaction 4				reaction 5				reaction 6			
method	ΔE_e	ΔE_0	ΔH_{298K}	ΔG_{298K}	ΔE_e	ΔE_0	ΔH_{298K}	ΔG_{298K}	ΔE_e	ΔE_0	ΔH_{298K}	ΔG_{298K}
B3LYP/6-31G*	16.0	11.5	12.5	9.1	−2.6	−6.4	−5.0	−16.2	−63.8	−59.3	−60.9	−53.8
B3LYP/6-31+G*	10.9	6.4	7.9	−3.4	−6.7	10.4	−9.1	−20.1	−53.5	−49.1	−50.6	−43.9
B3LYP/6-311++G**	5.9	1.6	3.1	−8.2	−11.1	−14.7	−13.4	−24.4	−43.9	−39.8	−41.4	−34.3
B3LYP/6-31G(2df,p)	11.6	7.4	8.8	−2.6	−6.5	−10.0	−8.7	−19.8	−53.4	−49.4	−51.0	−43.7
B3LYP/6-311+G(3df,2p)// B3LYP/6-31+G*	5.4	0.9	2.4	−9.0	−12.2	−15.9	−14.6	−25.6	−42.9	−38.4	−40.0	−33.3
MP2/6-311+G(3df,2p)// B3LYP/6-31+G*	10.9	6.4	7.9	−3.4	−10.0	−13.6	−12.3	−23..4	−39.2	−34.7	−36.3	−29.6
MP2/6-311+G(3df,2p)// B3LYP/6-31G(2df,p)	10.9	6.7	8.2	−3.3	−9.9	−13.5	−12.2	−23.2	−38.8	−34.8	−36.4	−29.1
G3MP2B3	10.2	5.9	7.4	−4.1	−9.9	−6.3	−8.6	−19.7	−40.7	−36.3	−37.9	−30.9
G4MP2	9.6	5.5	6.9	−4.5	−6.9	−10.4	−9.1	−20.2	−40.0	−36.02	−37.6	−30.4
G4	10.3	6.1	7.6	−3.9	−6.4	−9.9	−8.6	−19.6	−41.1	−37.1	−38.7	−31.5

[a] Reaction 1: glucose (A) → fructose (B), reaction 2: fructose (B) → fructose-1H_2O (enol, C) + H_2O, reaction 3: fructose-1H_2O (enol, C) ⇄ fructose-1H_2O (aldehyde, D) reaction 4: fructose-1H_2O (aldehyde, D) → fructose-2H_2O (E)+ H_2O, reaction 5: fructose-2H_2O (E) → fructose-3H_2O (HMF, F) + H_2O, reaction 6: HMF (F)+ 2H_2O → levulinic acid (G) + formic acid (H). [b] See Figure 1 for a schematic of the reaction pathway. The ΔE_e is the reaction energy from total electronic energies, ΔE_o is the reaction energy with zero-point energies included, ΔH_{298K} is the reaction enthalpy change at 298 K for the reaction, ΔG_{298K} is the reaction free energy change at 298 K.

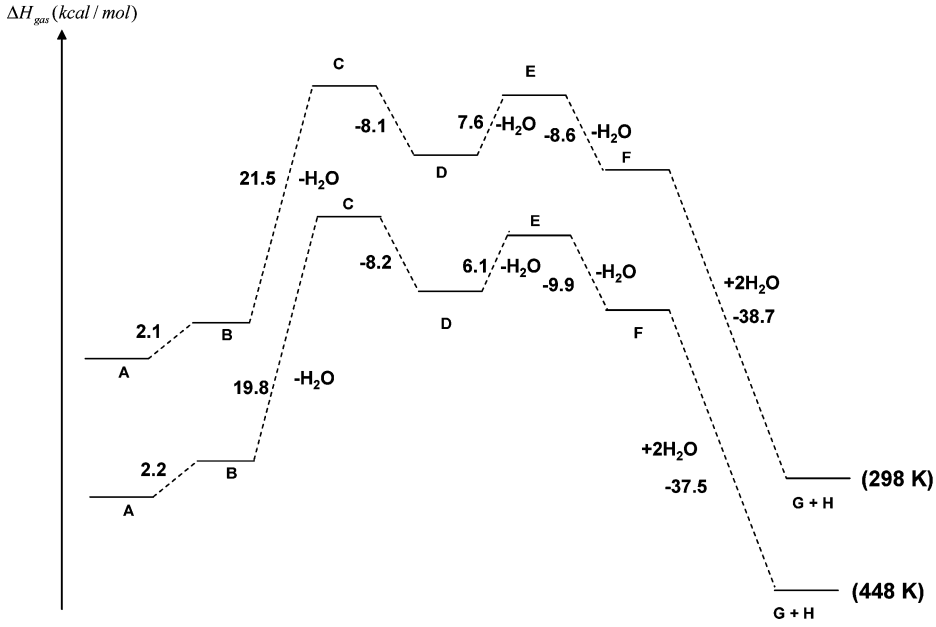

Figure 3. Schematic of enthalpy change during the reactions in Figure 1 calculated using G4 level of theory at 298 and 448 K in gas phase. Labels explained in Figure 1. The energies at 298 K and 448 K have been offset from one another for ease of viewing.

ization and initial elimination of a water molecule, the other reaction steps are thermodynamically favorable.

3.2. Solvation Effects on the Reaction Free Energies. The G4 free energies, with inclusion of solvation effects at 298 K, are given in parentheses in Figure 4. Accurate calculation of the effect of the reaction environment in determining the free energy of the reaction is a challenge in theoretical calculations. It has been reported that the aqueous solvation effects on sugar reactions are complicated due to the extensive hydrogen bond formation and intramolecular hydrogen bond network in the sugars.[14,37] In order to estimate the approximate effect of the aqueous medium on the reaction energies we have employed

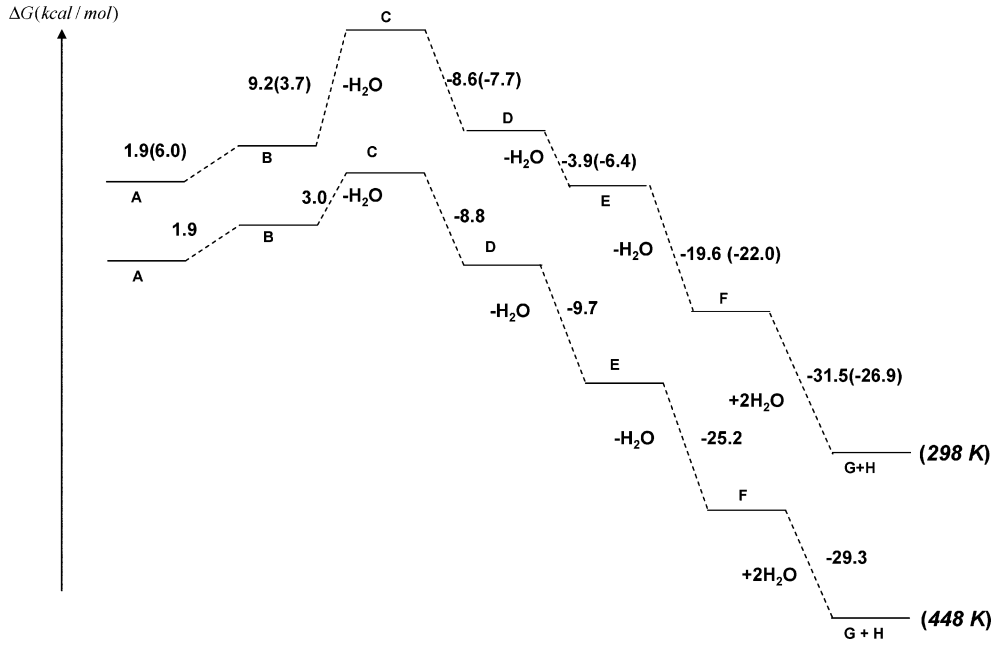

Figure 4. Schematic of free energy changes of the reactions in Figure 1 calculated using G4 level of theory at 298 K and 448 K. The values in parentheses are the G4 free energies at 298 K corrected for solvation effects calculated using CPCM at the B3LYP/6-31G(2df,p) level of theory with water as the solvent. Labels explained in Figure 1. The energies at 298 K and 448 K have been offset from one another for ease of viewing.

the polarizable continuum model described in the methods section and calculated the solvation energy changes at 298 K for the chemical transformations. The calculations indicate that glucose is stabilized in a water solvent by 4.1 kcal/mol over the fructose molecule. This is due to the fact that the glucose molecule is capable of more hydrogen bonding with surrounding water molecules because it has a higher solvent accessible surface area than fructose. Another notable change is the significant reduction, by 5.5 kcal/mol, in the free energy of the first dehydration process (**B** → **C**). This is because the enol molecule (**C**) is slightly more stabilized (1.4 kcal/mol) in aqueous solution than the fructose molecule (**B**) and, even more significantly, the water molecule removed from the fructose is stabilized (by 4.1 kcal/mol) in the aqueous environment. Thus, the calculated free energy change required to remove the first water molecule from fructose in aqueous reaction conditions is reduced to only +3.7 kcal/mol when solvent effects at 298 K are included (Figure 4). Similarly, subsequent dehydration processes are also favored by the stabilization of newly formed water molecules in the aqueous environments: by 2.5 and 2.4 kcal/mol, respectively, for the second and third dehydration processes. Overall, the solvation model gives a stabilization of −9.6 kcal/mol during the dehydration of fructose to HMF, suggesting that the dehydration process may be more favorable in aqueous conditions. The rehydration reaction (**F** → **G** +**H**) is destabilized by solvation (by 4.6 kcal/mol) due to consumption of two water molecules during the reaction.

A difficulty in converting glucose to HMF in aqueous solution is the stability of the pyranose forms of glucose over the furanose forms of fructose due to stabilization of pyranose forms in aqueous solution. Previous studies[6,38] suggest increased fructose concentrations in aprotic solvents such as DMSO due to the fact discussed above that the glucose molecule is capable of more hydrogen bonding with surrounding water molecules than fructose. Therefore, we have computed the solvation free energy change of all the reactions in DMSO ($\varepsilon = 46.8$) to compare with water ($\varepsilon = 78.4$). The free energy of the conversion of glucose to fructose is calculated to be very similar to that of the gas phase when using the DMSO dielectric (1.9 vs 2.1 kcal/mol) compared to that of the water dielectric (see Table S2 in the Supporting Information). This indicates the formation of furanosyl species is thermodynamically easier in aprotic solvents.

Another interesting aspect of these reactions is the effect of temperature on the reaction rate. It has been recently reported that dehydration of fructose to HMF proceeds faster at higher temperatures.[39] This could be due to either thermodynamic or kinetic factors. In this work, we have only considered the thermodynamic factors and the discussion that follows relates to these factors. The free energy landscape of the gas phase reactions at 448 K is shown in Figure 4. The gas phase free energy change for all dehydration steps becomes more negative with increasing temperature, with energy reductions of 6.2, 5.8, and 5.6 kcal/mol, respectively, for the first, second, third dehydration steps. The calculated free energy change for the rehydration process, on the other hand, was −29.3 kcal/mol at 448 K compared to −31.5 at 298 K. This suggests that at higher temperatures in aqueous solutions dehydration steps in the conversion of the fructose molecule will become more thermodynamically favorable while hydration steps will become less favorable. On the basis of thermodynamic considerations, the first dehydration step in conversion of glucose to levulinic is likely a key step in controlling the overall progress of the reaction due to its high endothermicity. Information on the kinetic factors is needed to make a definite conclusion concerning the rate determining step. The glucose to levulinic acid conversion is a very complicated reaction mechanism involving various hydration and dehydration steps that requires an additional detailed study to determine all activation barriers. Nimlos et al.[40] have reported calculated barriers for dehydration steps on a related reaction, conversion of xylose to furfural.

We note that even though the CPCM solvation model is able to qualitatively explain the relative solvation energy differences in the glucose decomposition reaction pathway, more accurate theoretical investigations are needed to quantitatively investigate the stabilization of different carbohydrate conformations and their hydrogen bonding networks.

TABLE 2: Comparison of Calculated Reaction Energies (ΔE_e, in kcal/mol) Using Other Functionals with Plane Wave and Gaussian Basis Sets[a]

	plane wave basis						
reaction	RPBE	PW91	PW91/BS1	PW91/BS3//PW91/BS1	PBE/BS3//PBE/BS1	B3PW91/BS2	G4
A → B (1)	1.9	1.7	1.7	1.9	1.9	2.2	2.6
B → C + H_2O (2)	12.4	20.5	26.3	19.6	19.0	21.8	24.3
C → D (3)	−5.2	−4.2	−9.2	−5.5	−5.6	−6.7	−7.8
D → E + H_2O (4)	1.2	7.9	12.5	7.3	6.8	9.7	10.3
E + → F + H_2O (5)	−16.2	−9.9	−5.1	−10.4	−11.0	−8.9	−6.4
F + 2H_2O→ G + H (6)	−34.8	−37.8	−53.7	−42.4	−42.3	−44.4	−41.1

[a] Reaction numbers from Table 1 given in parentheses. Other labels for the basis set are as follows: BS1: 6-31+G*; BS2: 6-31+G**; and BS3: 6-311+G(3dfp,2p).

3.3. Assessment of the Performance of Other Theoretical Methods. The G4 calculations for systems of size similar to glucose and fructose are computationally very demanding and, therefore, it is desirable to evaluate the performance of other methods for energy calculations involving sugar-related molecules, especially for use in future catalysis studies. In this section, we report on an assessment of various density functional methods, reduced perturbation *Gn* methods, and the MP2 method.

We have evaluated the energies of all the reactions in Figure 1 at the G4MP2, G3MP3B3, B3LYP/6-31G*, B3LYP/6-31+G*, B3LYP/6-311++G**, B3LYP/6-311+G(3df,2p)//B3LYP/6-31+G*, MP2/6-311+G(3df,2p)//B3LYP/6-31+G*, and MP2/6-311+G(3df,2p)//B3LYP/6-31G(2df,p), levels of theory. The calculated changes in electronic energy with (ΔE_0) and without zero-point energies (ΔE_e), enthalpy at 298 K (ΔH_{298K}) and free energy at 298 K (ΔG_{298K}) for all the reactions are tabulated in Table 1. One key result is the significant energy deviation (3−4 kcal/mol) of G3MP2B3 compared to G4 theory in predicting the energy difference between glucose and fructose and the reaction energy of the first dehydration step. This is mainly due to a geometry effect from the method where the B3LYP* level of theory is used for the geometry calculations. The geometry at this level of theory is inadequate to explain the energetics of the molecular systems similar to glucose. The G4 method uses B3LYP/6-31G(2df,p) geometries. This highlights the necessity of using more accurate geometries in such cases. The results in Table 1 also indicates that the G4MP2 method, which requires less time than G4 theory, gives results to within 1 kcal/mol of G4 theory.

Detailed analysis of the B3LYP and MP2 ΔE_e energies in Table 1 for the dehydration steps, in particular, shows ∼2−6 kcal/mol differences from the most accurate G4 reaction energies. Among the B3LYP methods in Table 1, B3LYP/6-31+G* and B3LYP/6-31G(2df,p) do the best with a maximum difference of about 2 kcal/mol for the G4 dehydration energies. However, these two methods differ from G4 theory by about 10 kcal/mol for the rehydration energy (reaction no. 6 in Table 1). The MP2/6-311+G(3df,p)//B3LYP/6-31+G*, MP2/6-311+G(3df,2p)/6-31G(2df,p) levels of theory perform very well in energy evaluations against the G4 calculations with a maximum difference of about 3 kcal/mol.

Due to an increase in interest in the theoretical calculations in catalysis of sugar molecules on surfaces, we have performed the reaction energetics calculations using plane wave basis sets to analyze their performance against the G4 method. Both the RPBE and PW91 functionals were tested, and the calculated reaction energies without zero-point energies are summarized in Table 2. In order to have a direct comparison, calculations using the PW91 functional with Gaussian basis sets were also performed. From Table 2, it is clear that the PW91 energies from the plane wave and 6-311+G(3df,2p) basis sets are in good agreement. The calculated PW91 energies are also in good agreement with the G4 results with the largest difference being about 5 kcal/mol for the first hydration step. The RPBE functional, however, has larger discrepancies for the energies of the dehydration steps with respect to G4 theory (9−12 kcal/mol). Interestingly, the offset between the PW91 and RPBE energies is very similar for each dehydration step. This offset in the RPBE energies may be due to an overestimate of the single bond to double bond conversion energy occurring in all three dehydration steps discussed earlier. The number of double bonds is conserved in the hydration step (HMF to levulinic acid and formic acid); in this case the RBPE energies are in good agreement with the higher level calculations. The PBE functional, from which RPBE is derived, performs well for the dehydration energies (differences of 1−2 kcal/mol with G4), when using appropriate basis set. Additionally, we have computed the energies using the B3PW91 functional and found that it has a maximum difference of 3 kcal/mol with respect to G4. Thus, of the functionals we have assessed PW91, B3PW91, and PBE give the best overall performance for the glucose decomposition reactions.

TABLE 3: Calculated Standard (298 K) Enthalpies of Formation (kcal/mol) at the G4 and G4MP2 Levels of Theory[a]

species	G4(MP2)	G4	expt.
A	−266.6	−268.9	
B	−264.3	−266.8	
C	−186.2	−187.9	
D	−194.1	−196.0	
E	−129.7	−131.0	
F	−81.2	−82.1	−79.8
G	−143.8	−144.9	
H	−90.2	−90.8	−90.4

[a] Labels of the species are explained in Figure 1.

3.4. Enthalpies of Formation. The enthalpies of formation of all the species in the glucose decomposition scheme (**A**−**H**, in Figure 1) were calculated using the G4 and G4MP2 methods at 298 K in the gas phase. The results are presented in Table 3. Due to the lack of gas phase experimental enthalpies of formation, the only comparison with experiment is possible for HMF and formic acid. Recently, Verevkin et al.[41] have reported an experimental enthalpy of formation for HMF of −79.8 ± 0.3 kcal/mol. The calculated standard enthalpy of formation of HMF at the G4 level of theory is −82.1 kcal/mol. This enthalpy of formation is based on the global minimum geometry and the other low energy conformations should be included for a more accurate value. On the basis of calculations of seven conformers by Verevkin et al.,[41] inclusion of the other conformers in a Boltzmann population distribution will make the G4

enthalpy of formation more positive by about 0.25 kcal/mol or about −81.8 kcal/mol, which is about 2 kcal/mol more negative than the experimental value. We note that the G4 method predicts an enthalpy of formation for furan and formic acid that are in very good agreement with experiment, with errors of only 0.1 and 0.4 kcal/mol, respectively. Verevkin et al.[41] also reported G3MP2 calculations and obtained a value of −81.6 kcal/mol for the enthalpy of formation of the global minimum energy conformer of HMF, which is close to the G4 value of 82.1 kcal/mol. By using three isodesmic reactions along with the G3MP2 enthalpy, they obtained a value of −79.8 for HMF, which is in agreement with their experimental value.

Accurate conformational analyzes of the molecular systems involved in this paper would require a detailed study due to the large number of conformations possible for species such as glucose and fructose. Momany et al.[12,28] have computed the geometries and energetics of the low lying conformations of glucose; among them twelve lowest energy conformers were selected and we have computed the Boltzmann population analysis (Table S3, Supporting Information). The computed correction value for the lowest energy conformer to incorporate the Boltzmann distribution is +0.34 kcal/mol.

Therefore, the enthalpies of formation in Table 3 are not likely to change much with the inclusion of conformer effects. Also it should not have a significant affect on the reaction energies for dehydration and rehydration.

4. Conclusions

In this work, we have presented a detailed thermochemical study of the conversion of glucose to levulinic acid through fructofuranosyl intermediates using the high-level ab initio methods G4 and G4MP2. The calculated gas phase reaction enthalpies indicate that the first two steps involving water molecule elimination are highly endothermic (by up to 22 kcal/mol), and the glucose to fructose conversion is very weakly endothermic (2 kcal/mol), while the other steps, including additional water elimination and rehydration to form levulinic acid, are exothermic (4 to 32 kcal/mol). The calculated gas phase free energies indicate that inclusion of entropic effects makes the dehydration steps more favorable, although the elimination of the first water remains endothermic by 9 kcal/mol at 298 K. Elevated temperatures and aqueous reaction environment are also predicted to make the dehydration reaction steps more thermodynamically favorable. On the basis of these enthalpy and free energy calculations, the first dehydration step in conversion of glucose to levulinic is likely a key step in controlling the overall progress of the reaction, although further studies of activation barriers are required for detailed understanding of the controlling factors and development of improved catalysts.

In an assessment of density functional theories based on the G4 energies, we have found that several functionals including PBE, PW91, and B3PW91 with appropriate basis sets perform quite well in predicting the energies (2−5 kcal/mol) of all of the reactions involved in the glucose decomposition reactions studied here. They may be useful in future investigations of catalysts for this process. Our study indicates that the B3LYP functional with the 6-31G* basis set performs well for the dehydration steps, but poorly for the rehydration steps, while the RPBE functional performs poorly for the dehydration steps.

The thermochemistry for glucose decomposition to levulinic acid provided by the accurate quantum chemical calculations described in this paper highlights the key steps and their thermodynamic feasibility, and hence provides a basis for further research in the catalysis of biomass. Design of a bifunctional catalyst, with the ability to control the dehydration and rehydration of species similar to glucose, would be vital to the design of effective new catalysts.

Acknowledgment. This work was supported by the U.S. Department of Energy under Contract DE-AC0206CH11357. This material is based upon work supported as part of the Institute for Atom-efficient Chemical Transformations (IACT), an Energy Frontier Research Center funded by the U.S. Department of Energy, Office of Science, Office of Basic Energy Sciences. We gratefully acknowledge grants of computer time from EMSL, a national scientific user facility located at Pacific Northwest National Laboratory, the ANL Laboratory Computing Resource Center (LCRC), and the ANL Center of Nanoscale Materials. We acknowledge helpful discussions with Prof. J. A. Dumesic.

Supporting Information Available: Thermochemistry of the reactions in the Figure 1 using additional levels of theory (Table S1), Free energy of the reactions at different solvent dielectrics (Table S2), details of Boltzmann conformational analysis (Table S3) and rederived high level correction parameters (Table S4). This material is available free of charge via the Internet at http://pubs.acs.org.

References and Notes

(1) Huber, G. W.; Chheda, J. N.; Barrett, C. J.; Dumesic, J. A. *Science* **2005**, *308*, 1446.
(2) Chheda, J. N.; Roman-Leshkov, Y.; Dumesic, J. A. *Green Chem.* **2007**, *9*, 342.
(3) Kunkes, E. L.; Simonetti, D. A.; West, R. M.; Serrano-Ruiz, J. C.; Gartner, C. A.; Dumesic, J. A. *Science* **2008**, *322*, 417.
(4) West, R. M.; Liu, Z. Y.; Peter, M.; Gartner, C. A.; Dumesic, J. A. *J. Mol. Catal A: Chem.* **2008**, *296*, 18.
(5) West, R. M.; Kunkes, E. L.; Simonetti, D. A.; Dumesic, J. A. *Catal. Today* **2009**, *147*, 115.
(6) Chheda, J. N.; Huber, G. W.; Dumesic, J. A. *Angew. Chem., Int. Ed.* **2007**, *46*, 7164.
(7) Csonka, G. I.; French, A. D.; Johnson, G. P.; Stortz, C. A. *J. Chem. Theory Comput.* **2009**, *5*, 679.
(8) Raju, R. K.; Ramraj, A.; Hillier, I. H.; Vincent, M. A.; Burton, N. A. *Phys. Chem. Chem. Phys.* **2009**, *11*, 3411.
(9) Appell, M.; Strati, G.; Willett, J. L.; Momany, F. A. *Carbohydr. Res.* **2004**, *339*, 537.
(10) Momany, F. A.; Appell, M.; Strati, G.; Willett, J. L. *Carbohydr. Res.* **2004**, *339*, 553.
(11) Appell, M.; Willett, J. L.; Momany, F. A. *Carbohydr. Res.* **2005**, *340*, 459.
(12) Momany, F. A.; Appell, M.; Willett, J. L.; Bosma, W. B. *Carbohydr. Res.* **2005**, *340*, 1638.
(13) Momany, F. A.; Appell, M.; Willett, J. L.; Schnupf, U.; Bosma, W. B. *Carbohydr. Res.* **2006**, *341*, 525.
(14) Ma, B. Y.; Schaefer, H. F.; Allinger, N. L. *J. Am. Chem. Soc.* **1998**, *120*, 3411.
(15) Cramer, C. J.; Truhlar, D. G. *J. Am. Chem. Soc.* **1993**, *115*, 5745.
(16) Xiang, Q.; Lee, Y. Y.; Torget, R. W. *Appl. Biochem. Biotechnol.* **2004**, *113−16*, 1127.
(17) Chang, C.; Ma, X. J.; Cen, P. L. *Chin. J. Chem. Eng.* **2006**, *14*, 708.
(18) Curtiss, L. A.; Redfern, P. C.; Raghavachari, K. *J. Chem. Phys.* **2007**, *127*, 124105.
(19) Baboul, A. G.; Curtiss, L. A.; Redfern, P. C.; Raghavachari, K. *J. Chem. Phys.* **1999**, *110*, 7650.
(20) Curtiss, L. A.; Raghavachari, K.; Redfern, P. C.; Rassolov, V.; Pople, J. A. *J. Chem. Phys.* **1998**, *109*, 7764.
(21) Curtiss, L. A.; Redfern, P. C.; Raghavachari, K. *J. Chem. Phys.* **2005**, *123*, 124107.
(22) Curtiss, L. A.; Redfern, P. C.; Raghavachari, K. *J. Chem. Phys.* **2007**, *126*, 084108.
(23) Curtiss, L. A.; Redfern, P. C.; Raghavachari, K.; Pople, J. A. *J. Chem. Phys.* **2001**, *114*, 108.
(24) Bylaska, E. J. Govind, W. A. d. J., N. Kowalski, K. Straatsma, T. P. Valiev, M. Wang, D. Apra, E. Windus, T. L. Hammond, J. Autschbach, J. Nichols, P. Hirata, S. Hackler, M. T. Zhao, Y. Fan, P.-D. Harrison, R. J.;

Smith, M. D., D. M. A. Nieplocha, J. Tipparaju, V. Krishnan, M.; Wu, A. V.-M., Q. Van Voorhis, T. Auer, A. A. Nooijen, M. Crosby, L. D. Brown, E. Cisneros, G. Fann, G. I. Fruchtl, H.; Hirao, J. G., K. Kendall, R. Nichols, J. A. Tsemekhman, K. Wolinski, K. Anchell, J. Bernholdt, D. Borowski, P. Clark, T. Clerc, D. Deegan, H. D.,M. Dyall, K. Elwood, D. Glendening, E. Gutowski, M. Jaffe, A. H., J. Johnson, B. Ju, J. Kobayashi, R. Kutteh, R. Littlefield, Z. L., R. Long, X. Meng, B. Nakajima, T. Niu, S. Rosing, L. P., M. Sandrone, G. Stave, M. Taylor, H. Thomas, G. Wong, J. v. L., A. Zhang. Z. NWChem, A Computational Chemistry Package for Parallel Computers, Version 5.1.1 (2009), Pacific Northwest National Laboratory, Richland, WA 99352−0999, USA. A modified version.

(25) Takano, Y.; Houk, K. N. *J. Chem. Theory Comput.* **2005**, *1*, 70.

(26) Cossi, M.; Rega, N.; Scalmani, G.; Barone, V. *J. Comput. Chem.* **2003**, *24*, 669.

(27) Barone, V.; Cossi, M. *J. Phys. Chem. A* **1998**, *102*, 1995.

(28) Bosma, W. B.; Schnupf, U.; Willett, J. L.; Momany, F. A. *J. Mol. Struc.: THEOCHEM* **2009**, *905*, 59.

(29) Perdew, J. P.; Chevary, J. A.; Vosko, S. H.; Jackson, K. A.; Pederson, M. R.; Singh, D. J.; Fiolhais, C. *Phys. Rev. B* **1992**, *46*, 6671.

(30) Hammer, B.; Hansen, L. B.; Nørskov, J. K. *Phys. Rev. B* **1999**, *59*, 7413.

(31) Perdew, J. P.; Burke, K.; Ernzerhof, M. *Phys. Rev. Lett.* **1996**, *77*, 3865.

(32) Becke, A. D. *J. Chem. Phys.* **1993**, *98*, 5648.

(33) Perdew, J. P.; Chevary, J. A.; Vosko, S. H.; Jackson, K. A.; Pederson, M. R.; Singh, D. J.; Fiolhais, C. *Phys. Rev. B* **1993**, *48*, 4978.

(34) Vanderbilt, D. *Phys. Rev. B* **1990**, *41*, 7892.

(35) Kresse, G.; Furthmuller, J. *Comput. Mater. Sci.* **1996**, *6*, 15.

(36) Frisch, M. J.; Trucks, G. W.; Schlegel, H. B.; Scuseria, G. E.; Robb, M. A.; Cheeseman, J. R.; Montgomery, J. A.; Vreven, T.; Kudin, K. N.; Burant, J. C.; Millam, J. M.; Iyengar, S. S.; Tomasi, J.; Barone, V.; Mennucci, B.; Cossi, M.; Scalmani, G.; Rega, N.; Petersson, G. A.; Nakatsuji, H.; Hada, M.; Ehara, M.; Toyota, K.; Fukuda, R.; Hasegawa, J.; Ishida, M.; Nakajima, T.; Honda, Y.; Kitao, O.; Nakai, H.; Klene, M.; Li, X.; Knox, J. E.; Hratchian, H. P.; Cross, J. B.; Bakken, V.; Adamo, C.; Jaramillo, J.; Gomperts, R.; Stratmann, R. E.; Yazyev, O.; Austin, A. J.; Cammi, R.; Pomelli, C.; Ochterski, J. W.; Ayala, P. Y.; Morokuma, K.; Voth, G. A.; Salvador, P.; Dannenberg, J. J.; Zakrzewski, V. G.; Dapprich, S.; Daniels, A. D.; Strain, M. C.; Farkas, O.; Malick, D. K.; Rabuck, A. D.; Raghavachari, K.; Foresman, J. B.; Ortiz, J. V.; Cui, Q.; Baboul, A. G.; Clifford, S.; Cioslowski, J.; Stefanov, B. B.; Liu, G.; Liashenko, A.; Piskorz, P.; Komaromi, I.; Martin, R. L.; Fox, D. J.; Keith, T.; Laham, A.; Peng, C. Y.; Nanayakkara, A.; Challacombe, M.; Gill, P. M. W.; Johnson, B.; Chen, W.; Wong, M. W.; Gonzalez, C.; Pople, J. A. *Gaussian 03, Revision C.02*, 2003.

(37) Molteni, C.; Parrinello, M. *J. Am. Chem. Soc.* **1998**, *120*, 2168.

(38) Roman-Leshkov, Y.; Chheda, J. N.; Dumesic, J. A. *Science* **2006**, *312*, 1933.

(39) Yao, C.; Shin, Y.; Wang, L. Q.; Windisch, C. F.; Samuels, W. D.; Arey, B. W.; Wang, C.; Risen, W. M.; Exarhos, G. J. *J. Phys. Chem. C* **2007**, *111*, 15141.

(40) Nimlos, M. R.; Qian, X.; Davis, M.; Himmel, M. E.; Johnson, D. K. *J. Phys. Chem. A* **2006**, *110*, 11824.

(41) Verevkin, S. P.; Emel'yanenko, V. N.; Stepurko, E. N.; Ralys, R. V.; Zaitsau, D. H.; Stark, A. *Ind. Eng. Chem. Res.* **2009**, *48*, 10087.

JP101418F